University College Cork, Ireland
Coláiste na hOllscoile Corcaigh

Identification of the transient stress-induced leakage current in silicon dioxide films for use in microelectromechanical systems capacitive switches

C. Ryan, Z. Olszewski, R. Houlihan, C. O'Mahony, A. Blake, and R. Duane

Identification of the transient stress-induced leakage current in silicon dioxide films for use in microelectromechanical systems capacitive switches

C. Ryan,[a] Z. Olszewski, R. Houlihan, C. O'Mahony, A. Blake, and R. Duane
Tyndall National Institute, University College Cork, Lee Maltings, Dyke Parade, Cork, Ireland

Dielectric charging at low electric fields is characterized on radio-frequency microelectromechanical systems (RF MEMS) capacitive switches. The dielectric under investigation is silicon dioxide deposited by plasma enhanced chemical vapor deposition. The switch membrane is fabricated using a metal alloy which is shown to be mechanically robust. In the absence of mechanical degradation, these capacitive switches are appropriate test structures for the study of dielectric charging in MEMS devices. Monitoring the shift and recovery of device capacitance-voltage characteristics revealed the presence of a charging mechanism which takes place across the bottom metal-dielectric interface. Current measurements on metal-insulator-metal devices confirmed the presence of interfacial charging and discharging transient currents. The field- and temperature-dependence of these currents is the same as the well-known transient stress-induced leakage current (SILC) observed in flash memory devices. A simple model was created based on established transient SILC theory which accurately fits the measured data and reveals that charge exchange at the bottom metal-dielectric interface is responsible for charging currents and pull-in voltage changes in these MEMS devices. © *2015 AIP Publishing LLC*. [http://dx.doi.org/10.1063/1.4919718]

Radio-frequency microelectromechanical systems (RF MEMS) capacitive switches are an enabling technology for future wireless communications with applications in phase shifters, impedance matching circuits, and software-defined radio.[1] Commercialization of these devices has been hindered by several reliability concerns which can cause the devices to fail under certain operating conditions. The moveable membrane of a capacitive switch is a key component for the tuning of microwave signals. Mechanical degradation of this membrane decreases the magnitude of all threshold voltages resulting in a narrowing of the device capacitance-voltage (CV) characteristic.[2–4] Another reliability concern is caused by the accumulation of charge inside the dielectric layer when an electric field stress is applied. As a result of dielectric charging the device CV curve will shift depending on the polarity of the dielectric charge.[5,6]

Monitoring the pull-in voltage shift is a commonly used method to characterize dielectric reliability.[7–11] It has been widely applied to different device architectures[9,11] fabricated using varied dielectrics[7,8,10] and processing conditions.[8,10] Dielectric charging of the intermetal dielectric of capacitive switches is most commonly studied; however, charging of the substrate layers in ohmic[12] and dielectricless capacitive[9] switches has also been reported. The evolution of pull-in voltage with stress time has been modeled by either exponential,[7] stretched exponential,[12–14] or power-law equations.[9,15]

Both the pull-in and release voltages of capacitive switches can be simultaneously affected by mechanical degradation and dielectric charging.[16] Therefore, it can be very difficult to isolate both mechanisms when only changes of the CV characteristic are used to characterize device reliability. However, an electrical test method has recently been developed,[3] which allows mechanical degradation to be studied in isolation using only changes in the CV curve.[16] A non-contact method has also been investigated to reduce the effect of mechanical degradation on dielectric charging measurements.[15] Dielectric charging will cause a shift of the voltage for capacitance minimum (V_{Cmin}), while this shift will be unaffected by mechanical degradation of the spring constant which causes CV narrowing.[2] However, mechanical degradation in the form of air gap change can affect V_{Cmin} measurements by changing the value of the minimum capacitance and therefore the calculated amount of charge.[4,13]

The devices used in this work are shunt capacitive switches fabricated over co-planar waveguide structures.[16] The substrate was composed of high-resistivity silicon wafers with $2 \mu m$ thick initial oxide deposited by plasma enhanced chemical vapor deposition (PECVD). The bottom electrode is a stack of two metal layers; $0.5 \mu m$ thick aluminum with $50 nm$ thick titanium nitride on top. The functional dielectric layer was PECVD SiO_2 deposited to a thickness of $130 nm$. A $3 \mu m$ thick polyimide sacrificial layer was spun and cured and a $1 \mu m$ thick metal alloy was deposited to form the membrane. The polyimide was then removed by oxygen plasma to release the switch.

Experiments were performed in a dry environment using a Cascade probe station, with various temperatures set via a thermal chuck and Temptronic temperature controller. DC bias voltages and CV sweeps were administered using an Agilent B1500 parameter analyzer equipped with a capacitance measurement unit. The use of a high-resolution semiconductor measurement unit allowed currents to be measured to a resolution of 2 fA; however, the noise level of the equipment was approximately 5 fA. Bipolar voltages were supplied to devices using an Agilent 81110 A pulse generator, where the signal was amplified to the required voltage using a high voltage amplifier. An

---

[a]Author to whom correspondence should be addressed. Electronic mail: cormac.ryan@tyndall.ie

Agilent 5250 A mainframe was used to switch between actuation and measurement equipment.

Following the method developed by Olszewski *et al.*,[3] a square-wave bipolar bias with a 50% duty cycle was used to mechanically stress the devices. The results of this mechanical stress are shown in Fig. 1 for two devices with different metal membranes.

Symmetric narrowing in the CV characteristic of an aluminum device was observed after 15 min of mechanical stress (Fig. 1(a)). This narrowing is caused by mechanical degradation of the switch membrane.[16] No change in the pull-in voltage was observed when the same mechanical stress was applied to a similar device fabricated using an aluminum alloy (Fig. 1(b)), demonstrating the excellent mechanical reliability of the membrane. Therefore, devices fabricated using this alloy were selected for the study of dielectric charging under the assumption that any variation in device characteristics could be attributed to dielectric charging only.

Fig. 2 shows the pull-in voltage change (ΔV_{PI}) of such a device under three different electrical stress conditions. In each case, a bias greater than the pull-in voltage was applied at the membrane to hold the device in the down-state. The bias was periodically turned off and CV sweeps were performed to monitor the ΔV_{PI}. After 60 min, the bias was removed and the device was allowed to recover in the up-state, while periodic CV sweeps were also performed to monitor the switch recovery. The device was allowed to completely recover before each subsequent measurement was performed. For a positive DC bias, the CV curve shifted to the left corresponding to negative charging of the dielectric. For a negative DC bias, the CV curve shifted to the right corresponding to positive charging of the dielectric. A bipolar bias with a 50% duty cycle was also applied to the device and no ΔV_{PI} was recorded after 1 h of bipolar stress, confirming that these devices are not subjected to mechanical degradation.
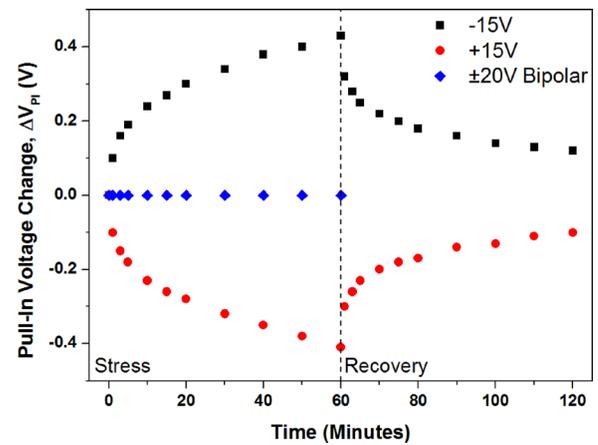
FIG. 2. Measured stress and recovery characteristics of a device undergoing three different electrical tests. Opposite and symmetric shifts are observed for +15 V and −15 V DC bias, and no change in V_{PI} is observed for ±20 V bipolar bias.

Since the same mechanical stress was applied to the device in each of the three tests, the effects of different electrical stresses on the ΔV_{PI} become clear. The bipolar signal succeeds in removing the effects of dielectric charging, resulting in zero V_{PI} shift. Pull-in voltage shifts of approximately equal magnitude but opposite direction are observed under DC biases of equal magnitude and opposite polarity. These results indicate that a bias polarity-independent charging mechanism is responsible for the CV shifts.

Dielectric discharging was also monitored by the recovery of the ΔV_{PI} once the DC bias had been removed. After 1 h of recovery, the V_{PI} returned to approximately 0.1 V of its initial value and fully recovered within several hours of relaxation. The stress and recovery characteristics show very similar behavior even though the membrane was not in contact with the dielectric during the recovery phase. These results strongly indicate that charging and discharging is taking place across the bottom metal-dielectric interface, similar to previously reported bulk charging mechanisms.[8,11]

It has been shown that the measurements of transient currents in MEMS and metal-insulator-metal (MIM) devices can reveal more information on charging processes.[14,17] Transient charging currents were measurable on our MEMS devices; however, it was not possible to record discharging currents once the bias had been removed and the membrane returned to the up-state. The measured charging currents were very low ($\approx$100 fA) and decayed to noise levels in approximately 10 s. Therefore, MIM devices were chosen for study, as these are similar to MEMS structures in the down-state but provide more reliable current measurements over longer time periods. The MIM devices were fabricated on a separate wafer while using the same PECVD oxide with a 0.5 μm thick aluminum bottom electrode and similar processing steps as the MEMS device in order to replicate their charging behavior as closely as possible.

Biases of both polarities were applied to the MIM top metal. Charging currents were measured at different dielectric fields and temperatures and were observed to possess a transient charging component which decayed over time as well as a constant, steady-state leakage current. Transient discharging currents were measured as soon as each bias had
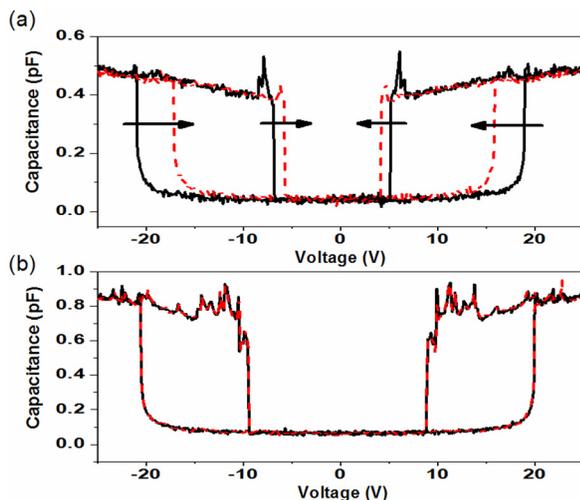

FIG. 1. (a) Measured capacitance-voltage characteristic at room temperature of a pure aluminum device before (solid black line) and after (dashed red line) mechanical stress. (b) Measured capacitance-voltage characteristic at room temperature of an aluminum alloy device before (solid black line) and after (dashed red line) mechanical stress.

been removed. Discharging current transients (DCTs) were chosen as the subject of the following investigation to avoid the influence of conduction currents on transient current measurements. Fig. 3(a) shows measured DCT current densities after the charging phase for a range of dielectric fields. Fig. 3(b) shows similar data for different temperatures at a dielectric field condition of 1.5 MV/cm.

Current measurements were performed after biasing MIM devices for 5 min with dielectric fields ranging from 0.2 to 1.5 MV/cm. The discharging current density increases with applied dielectric field. The polarity-independence of the process is evident in Fig. 3(a) as data for positive and negative polarities are approximately overlaid. This behavior is similar to what was observed on MEMS in Fig. 2 and suggests that the same mechanism may be responsible for charging and discharging in both cases. Temperature dependence of DCTs was also investigated after biasing with a dielectric field of 1.5 MV/cm. The devices were charged at different temperatures and the DCTs were recorded once the bias had been removed. In Fig. 3(b), the discharging current density is also observed to increase with temperature. The experimental data can be approximated by a single power-law over the full time range of the form

$$I(t) = I_0 t^{-m}, \tag{1}$$

where the time-dependence is based on the value of the exponent m, which can be extracted from the slope of a
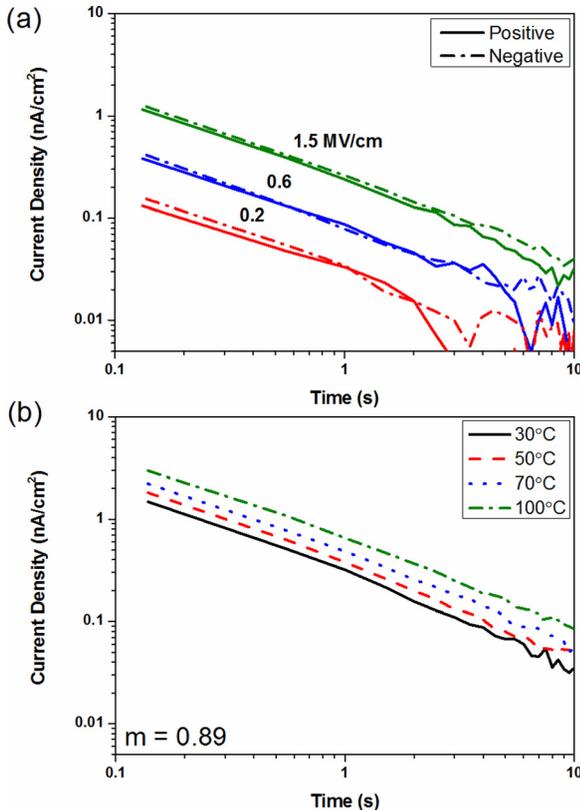

FIG. 3. Measured DCT current density vs. time plotted on a log scale. (a) DCTs measured after the device had been DC-biased for 5 min using different dielectric fields. (b) Measured DCTs for different temperatures after an applied dielectric field of 1.5 MV/cm. The average slope of the direct linear fitting of the log-log plot for all dielectric fields and temperatures (m = 0.89) is indicated on the graph.

straight line fit to the data when plotted on a log scale. Direct linear fitting was performed on the logarithmic data of Fig. 3 and an average exponent $m = 0.89$ was extracted across all measurements which, within measurement and fitting error limits, was observed to be approximately constant as a function of dielectric field strength and temperature. The extracted I_0 values are approximately linearly dependent on dielectric field strength and follow an Arrhenius relation over temperature with activation energy $E_A = 0.11$ eV.[18]

A similar power-law model with exponent close to 1 has previously been used to describe the transient stress-induced leakage current (SILC) observed in MOS and flash memory devices.[18,19] The affected dielectrics were typically high-quality thermal oxides with very low trap densities,[20,21] however, the SILC effect has also been observed in PECVD oxides.[22] The physical mechanism of the transient SILC effect has been modeled as the charging and discharging of border traps located within a few nm of metal-dielectric interfaces.[20,21] The border traps are present in the as-grown films and can also be generated during high field stress of the dielectric.[21]

To verify that the transient SILC effect is also present in the MEMS devices and affects device operation, a simple model is proposed to explain the ΔV_{PI} measured in our MEMS devices at low electric fields. During the charging phase, we assume that no charge is trapped near the top metal-dielectric interface due to rough contact between the two materials, where fewer contact points limit the possibility for charge exchange.[4] Based on our measurements and transient SILC theory, we assume that all trapped charge is located in close proximity to the bottom metal-dielectric interface such that the charge can easily be exchanged through the bottom metal. Modeling the trapped charge $Q_{Trapped}$ as a uniform charge sheet with centroid located at position z, the charge distribution on the MEMS device in the down-state can be drawn as in Fig. 4(a). In this case, negative charge is assumed to be trapped in the dielectric with positive induced charge on the electrodes. In the down-state, the MEMS device resembles a parallel plate capacitor where the trapped charge density has induced charges on the top and bottom electrodes so that the capacitor is electrically neutral. Using Gauss' law, it can be shown that[23]

$$Q_{Top} = -\frac{z}{t_{ox}} Q_{Trapped}, \tag{2}$$

where the oxide thickness t_{ox} is the distance between the two plates and Q_{Top} is the induced charge on the top electrode. Under an applied bias, charge tunnels from the bottom electrode into the dielectric forming a trap layer at depth z. The induced charge on the top electrode is supplied by the external circuit such that

$$I_{meas} = \frac{d}{dt}\left(-\frac{z}{t_{ox}} Q_{Trapped}\right). \tag{3}$$

During the discharging phase in MEMS devices, the membrane is in the up-state and the effective thickness of the capacitor increases to $t_{ox} + \varepsilon_d t_{air}$ which will significantly reduce the induced charge Q_{Top}. This explains why discharging currents were not measurable on our MEMS devices.
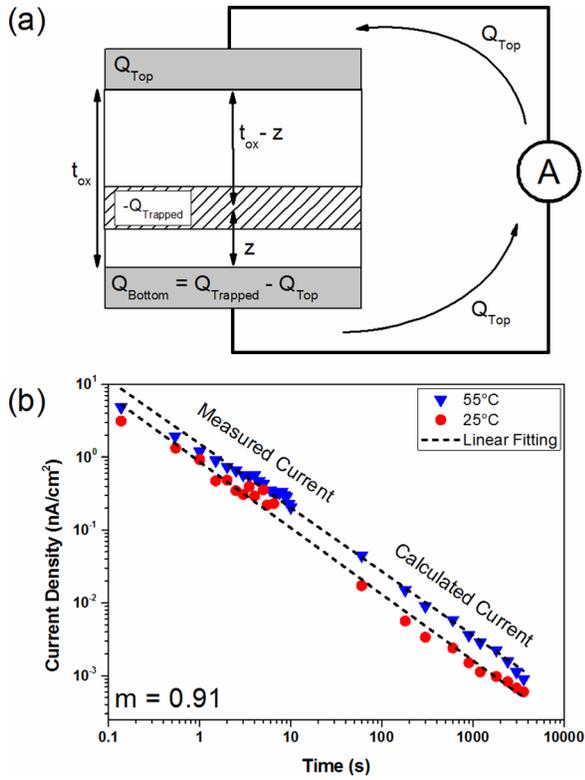
FIG. 4. (a) Model of the charge distribution on a MEMS device in the down-state assuming perfect contact between metal and dielectric. (b) Measured charging currents with an applied field of 3 MV/cm and calculated charging currents from Eq. (5) using measured ΔV_{PI}. Measurements were repeated for a range of dielectric fields between 1.5 MV/cm and 3 MV/cm and at 10 °C and 40 °C but are not shown for clarity. The average slope of the direct linear fitting of the log-log plot for all dielectric fields and temperatures (m = 0.91) is indicated on the graph.

By monitoring the ΔV_{PI} over time, the amount of trapped charge in the dielectric can be calculated using a model analogous to the model derived by Wibbeler *et al.*[6]

$$Q_{Trapped} = \frac{\varepsilon_0 \varepsilon_d A}{z} \Delta V_{PI}, \qquad (4)$$

where A is the device area, ε_0 and ε_d are the permittivities of air and the dielectric, respectively, and the position of the charge centroid z is measured with respect to the bottom metal-dielectric interface. In our devices, a typical ΔV_{PI} of 0.6 V corresponds to a trap density of states $N_{it} = 6.45 \times 10^{12}$ cm^{-2} if the trap centroid is located at a depth of 2 nm. Combining Eqs. (2) and (4) results in an expression which can be used to calculate the charging current in a MEMS device based on the measured ΔV_{PI}

$$I_{meas} = -\frac{\varepsilon_0 \varepsilon_d A}{t_{ox}} \frac{d}{dt} \Delta V_{PI} = -C_{ox} \frac{d}{dt} \Delta V_{PI}. \qquad (5)$$

Note that (5) is independent of the position of the charge centroid and the remaining physical constants equate to the oxide capacitance C_{ox}. While the theoretical down-state capacitance of our devices is 2.6 pF the measured value of C_{ox} was recorded at 0.8 pF due to roughness of the top contact.

The ΔV_{PI} of a MEMS device was measured over 1 h of DC bias and using Eq. (5) charging currents were calculated. Charging currents were also measured at the bottom metal

during the first ten seconds of stress until the noise floor of the equipment was reached. Measurements were performed for a range of temperatures and low dielectric fields (≤ 3 MV/cm) but for clarity only two sets of results at 25 °C and 55 °C for a dielectric field of 3 MV/cm are shown in Fig. 4(b). The range of dielectric field conditions was limited between 1.5 and 3 MV/cm to ensure device actuation but maintain a sufficiently low dielectric field. A maximum temperature of 55 °C was chosen to minimize any potential mechanical degradation effects which are accelerated by temperature.[24] The MEMS charging current transients exhibit similar behavior to MIM device currents and can also be approximated by a single power-law process with an average exponent m = 0.91, which, within measurement and fitting error limits, is approximately constant as a function of dielectric field strength and temperature. The extracted I_0 values are also approximately linearly dependent on dielectric field strength and follow an Arrhenius relation over temperature with activation energy $E_A = 0.14$ eV. The excellent agreement between measured data and the model (5) establishes that charge exchange at the bottom metal-dielectric interface is responsible for the charging currents and ΔV_{PI} in our MEMS devices. Furthermore, it can be concluded that any top metal-dielectric interfacial charging which occurs in our devices is not significant.

Transient SILC experiments have demonstrated power-law charging and discharging processes with exponents which are independent of charging bias magnitude and polarity[25] but which are dependent on the trap distribution in the dielectric.[19] For instance, it was shown that the exponent changes after a high-field (>5 MV/cm) stress which causes additional traps to be generated in the dielectric.[21] Given that our devices are not exposed to such high field stresses (≤ 3 MV/cm) and that repeated measurements on MIM and MEMS devices have shown little change in the power-law exponent with charging bias, polarity, or temperature, we conclude that no new traps are generated in the oxide and that the transient current behavior and changes in pull-in voltage are due to the charging and discharging of existing border traps located close to the bottom metal dielectric interface. The charging and discharging of the border traps have been explained by both elastic[18,19] and inelastic tunneling processes.[21,26] According to the elastic tunneling front model[27] and assuming a uniform spatial distribution of traps, the trapped charge is assumed to be initially adjacent to the metal-dielectric interface and moving into the dielectric at the rate of approximately 0.2–0.4 nm per decade of time.[28] As the process is limited by tunneling from the bottom metal,[21] the position of the charge centroid is expected to be situated within a few nm of the bottom metal-dielectric interface.[29]

Mechanically robust RF MEMS capacitive switches were fabricated to study the effects of dielectric charging in PECVD silicon dioxide. Under low electric fields, a charging process was found to occur through the bottom metal-dielectric interface. Measurements on MIM devices revealed the presence of transient currents with the same behavior as the well-known transient SILC effect in MOS and flash memory devices. The excellent agreement between a simple model and experimental results on MEMS devices confirms that charging and discharging of border traps at the bottom metal-dielectric interface is

responsible for the observed dielectric charging at low electric fields in our MEMS technology.

[1]H. J. De Los Santos, *RF MEMS Circuit Design for Wireless Communications* (Artech House, Boston, USA, 2002).

[2]R. W. Herfst, P. G. Steeneken, and J. Schmitz, paper presented at the IEEE 21st International Conference on Micro Electro Mechanical Systems (MEMS), 13–17 January 2008.

[3]Z. Olszewski, R. Houlihan, C. Ryan, C. O'Mahony, and R. Duane, Appl. Phys. Lett. **100**(23), 233505 (2012).

[4]Z. Olszewski, R. Houlihan, C. O'Mahony, and R. Duane, Appl. Phys. Lett. **100**(2), 029903 (2012).

[5]J. R. Reid and R. T. Webster, Electron. Lett. **38**(24), 1544–1545 (2002).

[6]J. Wibbeler, G. Pfeifer, and M. Hietschold, Sens. Actuators, A **71**(1–2), 74–80 (1998).

[7]X. B. Yuan, Z. Peng, J. C. M. Hwang, D. Forehand, and C. L. Goldsmith, IEEE Trans. Device Mater. Reliab. **6**(4), 556–563 (2006).

[8]Z. Peng, C. Palego, J. C. Hwang, D. I. Forehand, C. L. Goldsmith, C. Moody, A. Malczewski, B. W. Pillans, R. Daigler, and J. Papapolymerou, IEEE Microwave Wireless Compon. Lett. **19**(5), 299–301 (2009).

[9]D. Mardivirin, A. Pothier, A. Crunteanu, B. Vialle, and P. Blondy, IEEE Trans. Microwave Theory Tech. **57**(1), 231–236 (2009).

[10]D. Molinero and L. Castañer, Appl. Phys. Lett. **92**(4), 043502 (2008).

[11]D. Molinero, C. Shen, J. Hwang, A. Stamper, S. Cunningham, and A. Morris, in 2013 Transducers & Eurosensors XXVII: The 17th International Conference on Solid-State Sensors, Actuators and Microsystems (TRANSDUCERS & EUROSENSORS XXVII) (2013).

[12]R. Marcelli, G. Papaioannu, S. Catoni, G. De Angelis, A. Lucibello, E. Proietti, B. Margesin, F. Giacomozzi, and F. Deborgies, J. Appl. Phys. **105**(11), 114514–114524 (2009).

[13]M. S. Koutsoureli and G. J. Papaioannou, Microelectron. Reliab. **51**(9–11), 1874–1877 (2011).

[14]M. Koutsoureli and G. Papaioannou, Appl. Phys. Lett. **99**(10), 103503 (2011).

[15]R. W. Herfst, P. G. Steeneken, and J. Schmitz, paper presented at the 45th Annual IEEE International Reliability Physics Symposium, 15–19 April 2007.

[16]C. Ryan, Z. Olszewski, R. Houlihan, C. Mahony, and R. Duane, Appl. Phys. Lett. **104**(6), 061908 (2014).

[17]D. Molinero and L. Castaner, Appl. Phys. Lett. **96**(18), 183503 (2010).

[18]R. Moazzami and H. Chenming, paper presented at the Technical Digest - International Electron Devices Meeting (IEDM), 13–16 December 1992.

[19]D. J. Dumin and J. R. Maddux, IEEE Trans. Electron Devices **40**(5), 986–993 (1993).

[20]E. F. Runnion, S. M. Gladstone, R. S. Scott, Jr., D. J. Dumin, L. Lie, and J. C. Mitros, IEEE Trans. Electron Devices **44**(6), 993–1001 (1997).

[21]D. Ielmini, A. S. Spinelli, M. A. Rigamonti, and A. L. Lacaita, IEEE Trans. Electron Devices **47**(6), 1258–1265 (2000).

[22]B. Wood, B. McDougall, O. Chan, A. Dent, C.-N. Ni, R. Hung, H. Chen, P. Xu, P. Nguyen, and M. Okazaki, ECS Trans. **35**(2), 69–81 (2011).

[23]R. S. Muller, *Device Electronics for Integrated Circuits*, 3rd ed. (John Wiley & Sons, New York, NY, 2003).

[24]M. McLean, W. L. Brown, and R. P. Vinci, J. Microelectromech. Syst. **19**(6), 1299–1308 (2010).

[25]R. S. Scott and D. J. Dumin, paper presented at the 1995 International Conference on Microelectronic Test Structures, ICMTS, 22–25 March 1995.

[26]S. Takagi, N. Yasuda, and A. Toriumi, IEEE Trans. Electron Devices **46**(2), 335–341 (1999).

[27]F. P. Heiman and G. Warfield, IEEE Trans. Electron Devices **12**(4), 167–178 (1965).

[28]T. R. Oldham, A. J. Lelis, and F. B. McLean, IEEE Trans. Nucl. Sci. **33**(6), 1203–1209 (1986).

[29]A. S. Spinelli, A. L. Lacaita, M. Rigamonti, and G. Ghidini, IEEE Electron Device Lett. **20**(3), 106–108 (1999).